Clays and Clay Minerals, Vol. 53, No. 1, 92–99, 2005.

MICROSCOPY STUDIES OF THE PALYGORSKITE-TO-SMECTITE TRANSFORMATION

MARK P. S. KREKELER[1,*], ERIC HAMMERLY[2], JOHN RAKOVAN[2] AND STEPHEN GUGGENHEIM[3]

[1] Department of Environmental Science and Policy, George Mason University, Fairfax, Virginia, 22030 USA
[2] Department of Geology, Miami University, Oxford, Ohio, 45056 USA
[3] Department of Earth and Environmental Sciences, University of Illinois at Chicago, Chicago, Illinois, 60607 USA

Abstract—The transformation process between palygorskite and smectite was studied by examining the morphological and structural relationships between these two minerals in an assemblage from the Meigs Member of the Hawthorne Formation, southern Georgia. Studied samples were related to an alteration horizon with a tan clay unit above and a blue clay unit below. Atomic force microscopy (AFM) and transmission electron microscopy (TEM) were used to study the mechanism of transformation.

From AFM data, both clay units contain euhedral palygorskite fibers. Many fibers are found as parallel intergrowths joined along the [010] direction to form 'raft-like' bundles. Degraded fibers, which are common in the tan clay, have a distinctly segmented morphology, suggesting a dissolution texture. Many of the altered palygorskite fibers in the tan clay exhibit an oriented overgrowth of another mineral phase, presumably smectite, displaying a platy morphology. This latter mineral forms along the length of the palygorskite crystals with an interface parallel to {010} of the palygorskite. The resulting grain structures have an elongate 'wing-like' morphology.

Imaging by TEM of tan clay material shows smectite lattice-fringe lines intergrown with 2:1 layer ribbon modules (polysomes) of the palygorskite. These features indicate an epitaxial overgrowth of smectite on palygorskite and illustrate the structural relationship between platy overgrowths on fibers observed in AFM data. The epitaxial relationship is described as {010} [001] palygorskite || {010} [001] smectite.

Energy dispersive spectroscopy indicates that the smectite is ferrian montmorillonite. Polysomes of palygorskite fibers involved in these textures commonly vary and polysome widths are consistent with double tetrahedral chains (10.4 Å), triple tetrahedral chains (14.8 Å), quadruple tetrahedral chains (21.7 Å) and quintuple tetrahedral chains (24.5 Å).

The transformation of palygorskite to smectite and the resulting intergrowths will cause variations in bulk physical properties of palygorskite-rich clays. The observation of this transformation in natural samples suggests that this transformation mechanism may be responsible for the lower abundance of palygorskite in Mesozoic and older sediments.

Key Words—Atomic Force Microscopy, Epitaxy, Palygorskite-sepiolite, Phase Transformation, Smectite, Transmission Electron Microscopy.

INTRODUCTION

Palygorskite and sepiolite are modulated phyllosilicates that may be described as consisting of polysomes of 2:1 layer ribbons, which are connected by inverted silicate tetrahedra. Although these layer ribbons are infinite in one direction, they may be considered modular units that can vary in one dimension, along the ribbon width. Thus, the layer ribbon or polysome can be used to describe a continuously variable structure depending on how the ribbon widths vary.

Sedimentary deposits of palygorskite-sepiolite minerals are important geologically because they represent specific depositional environments characterized by elevated salinities and pH conditions (Jones and Galán, 1988). Formation of palygorksite-sepiolite minerals at near-neutral pH or in diluted groundwaters has also been suggested in arid settings in closed basins (Leguey *et al.*, 1995; Khoury *et al.*, 1982). Although large sedimentary deposits of palygorskite-sepiolite minerals are known to occur, they are uncommon in rocks older than the Middle Tertiary and this temporal restriction may be related to possible transformations of palygorskite to smectite. Palygorskite-sepiolite minerals are also of industrial interest because of their sorption capacity and catalytic behavior. They are used mainly as an absorbent for pet wastes or oils and greases, and as a component of drilling muds (Galán, 1996). Properties of palygorskite clays used in these applications are often variable. One mechanism that may affect bulk properties of these clays is the physiochemical transformation of palygorskite to smectite. The occurrence of partially altered palygorskite fibers or palygorskite-smectite aggregate particles can considerably affect the microfabric of natural samples, thereby reducing its value as an industrial sorbent.

The transformation of palygorskite to smectite has been considered by Golden and Dixon (1990), Merkl

* E-mail address of corresponding author:
mkrekele@gmu.edu
DOI: 10.1346/CCMN.2005.0530109

Copyright © 2005, The Clay Minerals Society

https://doi.org/10.1346/CCMN.2005.0530109 Published online by Cambridge University Press

(1989), Golden *et al*. (1985), Güven and Carney (1979) and Randall (1956). Merkl (1989) identified textural relationships of smectite, kaolinite and palygorskite in the Meigs Member and the Dogtown Clay Member of the Hawthorne Formation in southern Georgia. His work suggested that a transformation may exist between palygorskite and smectite, although the scanning electron microscopy (SEM) data were not of sufficient resolution to describe any transformation in detail. Merkl (1989) obtained SEM images showing that palygorskite strands broaden upon initial alteration, followed by additional broadening and coalescence into irregular sheets of smectite. Güven and Carney (1979) investigated hydrothermal reactions in the sepiolite-water system in the presence of NaCl and other salts and hydroxides. They found that NaCl increased the rate of formation of stevensite at temperatures below 260ºC, and from 260 to 316ºC sepiolite readily converted to stevensite independent of the ionic strength of the solution. Golden *et al*. (1985) produced smectite from palygorskite by reactions with solutions at 150ºC. Transmission electron microscopy images of grain mounts showed alteration and corrosion textures of palygorskite fibers and an intimate relationship of smectite with reacted palygorskite fibers. They suggested that a dissolution-reprecipitation process occurred, although a solid-state transformation could not be ruled out. Golden and Dixon (1990) showed that palygorskite readily converted to smectite at temperatures above 100ºC, although the reaction was sluggish at room temperature (22ºC). Experiments conducted near a pH of 12 showed that the palygorskite-to-smectite transformation occurs over a period of a few months. Their TEM images of grain mounts indicate a close textural association of smectite and palygorskite.

The purpose of this paper is to examine the morphological and structural relationships between palygorskite and smectite in a natural clay assemblage using AFM and TEM to understand better the transformation process between these two minerals. Atomic force microscopy provides detailed information regarding particle morphology and TEM imaging can provide information regarding the microfabric and structural relationships between mineral transformations. Although previous workers have shown an intimate association of particles of palygorskite-sepiolite and smectite, the details regarding the nature of this association are unclear. For example, it is uncertain in TEM images obtained from grain mounts whether or not smectite particles are simple aggregates associated with palygorskite-sepiolite fibers.

GEOLOGICAL SETTING AND PREVIOUS WORK

The Middle Miocene Hawthorne Group in southern Georgia is part of the Meigs-Attapulgas-Quincy industrial mineral district of Georgia and Florida (Patterson, 1974). The bulk mineralogy and sedimentology of the palygorskite deposits of the Hawthorne Formation were studied previously by powder X-ray diffraction (XRD) methods (Merkl, 1989; Weaver, 1984; Weaver and Beck, 1977; Patterson, 1974) and a combination of powder XRD and SEM techniques (Merkl, 1989). The deposits occur as discontinuous beds in either the Dogtown Clay Member (Torreya Formation) or the Meigs Member (Merkl, 1989). The Meigs Member is composed of short-length palygorskite (2−5 μm), smectite, sepiolite, opal-A, opal-CT and trace amounts of clinoptilolite (Merkl, 1989). The deposits formed in shallow marine lagoons, tidal flats or ephemeral lakes under subtropical conditions (Patterson, 1974; Merkl, 1989). Patterson (1974) argued that the Mg in the authigenic clays originated from evaporating seawater, and that Si and Al were introduced by streams flowing into the basins. Merkl (1989) suggested that precursor kaolinite and smectite transformed in the alkaline basins to smectite and palygorskite, possibly via a neoformation process (*i.e.* chemical precipitation in a sedimentary environment).

Merkl found that a sharp contact defines an alteration horizon consisting of a tan clay unit that overlies a blue clay unit in the Meigs member of the Hawthorne Formation at the Pittman Quarry near the town of Ocklocknee, Georgia. Although not formally defined as stratigraphic units, these beds are hereafter referred to as 'tan clay', and 'blue clay', respectively. The origin of these units is suggested by Merkl (1989) to reflect "roll front type weathering" and the color difference is believed to be related to a paleohydrologic interface. The tan clay is thought to result from the spatial extent of a vadose zone, permitting oxidation of minerals and the formation of Fe oxides, whereas the blue clay reflects a phreatic zone. Krekeler *et al*. (2004) found that palygorskite is the dominant phyllosilicate present in both clay units. Lesser amounts of smectite, illite, kaolinite and interstratified illite-smectite also occur. A 'bird's-nest' fabric, which consists of interwoven palygorskite fibers that cross each other in three-dimensional arrays, is dominant and comprises ~90 to 95% of the palygorskite fabric in both the tan and blue clays (Krekeler *et al*., 2004). The remaining fabric (5−10%) involves close, compact parallel palygorskite fibers that are found locally and appear to be filling void space between fibers comprising the bird's-nest texture. The blue clay generally has thin fibers ~20 nm in diameter whereas the tan clay has fibers that vary in width between 20 and 40 nm. One component of the formation of the tan clay through weathering or alteration is the speculated transformation of palygorskite to smectite (Merkl, 1989), which is the focus of this study.

MATERIALS AND METHODS

Samples

Samples from a fresh exposure from the Meigs Member were collected systematically on both sides of

https://doi.org/10.1346/CCMN.2005.0530109 Published online by Cambridge University Press

the (horizontal) alteration contact separating the tan and blue clays, ~200 m from the location sampled by Merkl (1989). Sample collection was essentially perpendicular (near vertical) to the contact, and a continuous section was taken from ~1.5 m above the contact to ~2 m below it at 5 cm intervals. Samples were placed in sealed rigid containers to preserve texture. Small chips 0.5–1.0 cm in diameter were taken from selected samples for AFM and TEM study.

AFM sample preparation

For examination using AFM, clay samples from above and below the boundary were prepared using gentle sonication in water to create a colloidal suspension. Approximately 0.01 g of each sample was added to ~15 mL of deionized water, and then sonicated for 15 min. This sonication process is sufficiently vigorous to disaggregate the clay particles but sufficiently gentle to preserve morphological features and intergrowth textures of the clays. Using a calibrated pipette, 0.05 mL of each colloid was placed on a freshly cleaved mica substrate that was glued to a stainless steel AFM puck. Samples were then covered to prevent excessive contamination by adventitious material and allowed to dry thoroughly for 24 h. Upon drying, the clays adhere tightly on the mica surface and cannot be moved by the AFM tip.

The AFM data were collected in open-air conditions on a Digital Instruments Nanoscope IIIa MultiMode AFM, in TappingMode® using TESP silicon probes. This microscope configuration has routinely produced nm resolution of clay minerals (Nagy and Blum, 1994; Bickmore *et al.*, 2001) and is an ideal technique for measuring micromorphological features.

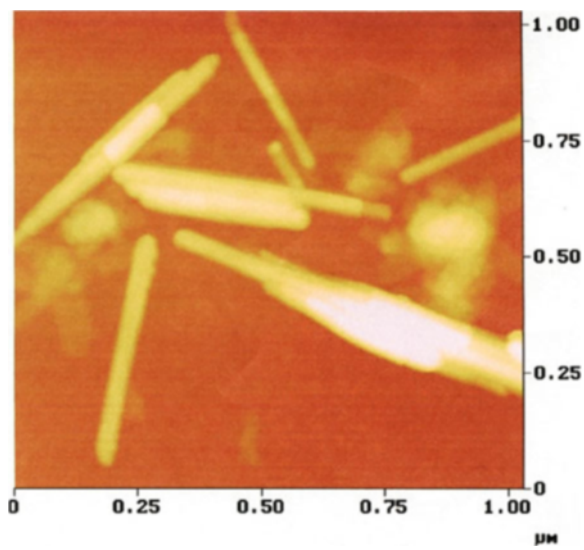


Figure 1. AFM image (height data) of the blue clay dispersed on a mica substrate. The euhedral, acicular crystals are palygorskite. The tabular, pseudohexagonal crystals are other layer silicates.

TEM sample preparation

Samples were prepared for TEM study using a technique modified from Kim *et al.* (1995), and a detailed description is given by Krekeler *et al.* (2004). In summary, the procedure involves the use of London Resin White (LRW) to infiltrate the sample chip over time with sequentially higher concentrations of resin. The final step involves the addition of an accelerant to polymerize the sample. Because the sample chips in this study were large, the procedure took ~11 weeks, instead of ~1 week used by Kim *et al.* (1995).

Thin-sections were produced, and 3 mm Cu grids were prepared. Grids were ion milled to produce perforations at a glancing angle of 22° using a Gatan ion mill. The TEM analyses were obtained using a 300 kV JEOL JEM-3010 transmission electron microscope equipped with an ultra-high-resolution pole piece, resulting in a point-to-point spatial resolution of 0.17 nm. A 20 μm objective aperture was used for bright field imaging. Images were captured electronically using a Gatan CCD imaging system. Energy dispersive spectra (EDS) were obtained using a Noran EDS system.

RESULTS

Atomic force microscopy

Samples from the blue and tan clays display several features that are in striking contrast to each other. In the blue clay, where, after initial deposition, it is speculated that limited reactions with oxidizing meteoric groundwaters have occurred; the palygorskite fibers exhibit the

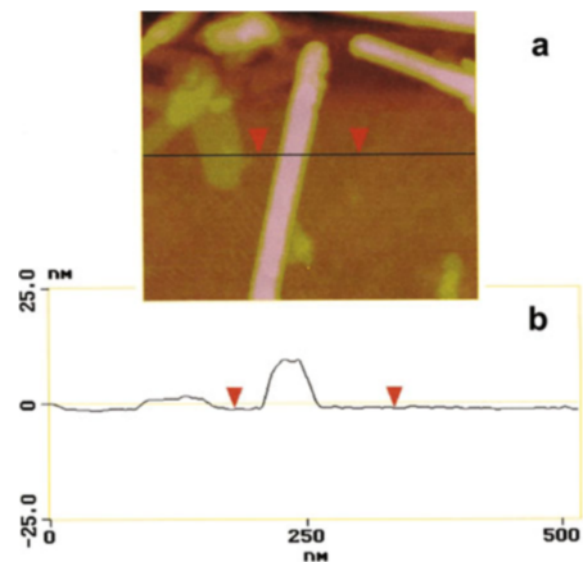


Figure 2. (a) AFM image (height data) of the blue clay dispersed on a mica substrate. The area shown is from the lower left quadrant of Figure 1. (b) Cross-sectional view of data along the black line in a.

https://doi.org/10.1346/CCMN.2005.0530109 Published online by Cambridge University Press

euhedral, acicular habit that is characteristic of this mineral (Figures 1,2). Distinct, well-formed individual crystals displaying a flat, tabular habit (Figures 1,2) characteristic of other layer silicates are also observed. These platy particles were not specifically associated with or connected to palygorskite fibers. Instead, the platy particles were found randomly oriented and distributed throughout the sample. Anhedral material was also observed amongst the morphologically well developed crystals.

Samples from the tan clay show a combination of characteristic, euhedral palygorskite, and partially degraded fibers that exhibit a distinctly segmented morphology suggestive of a dissolution texture (Figures 3,4). The degraded, hummocky microtopography that is dominant in the tan clay samples is distinct from the microtopography of blue clay samples. Well formed, euhedral crystals with low surface microtopography, characteristic of the blue clay are replaced by rough-edged, hummocky crystals with much greater surface microtopography. Although still displaying an elongate habit, palygorskite fibers from the tan clay have an average length (400 nm) that is shorter than those in the blue clay (750–1000 nm) samples.

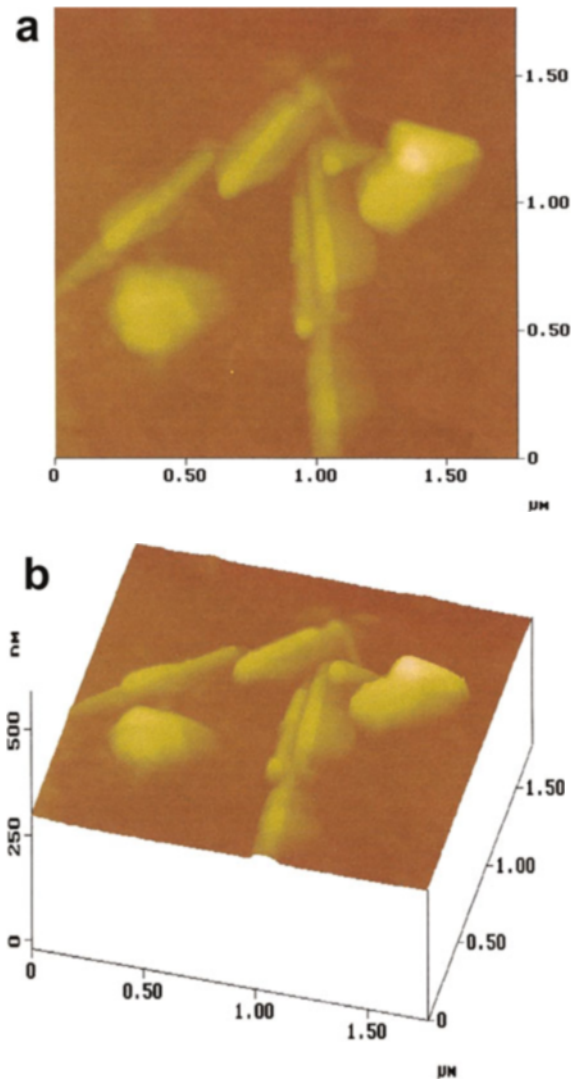


Figure 3. (a) AFM image (height data) of the tan clay dispersed on a mica substrate (plan view). Acicular crystals are palygorskite with 'wing-like' overgrowths of smectite. The hexagonal crystal in the lower left part of the image also shows an overgrowth of a morphologically similar phase. This may be smectite on kaolinite as was described by Krekeler *et al.* (2004). (b) Three-dimensional AFM image (height data) of the same scan.

Many of the altered palygorskite fibers in the tan clay also exhibit an oriented overgrowth of another mineral phase displaying a platy morphology (Figures 3,4). This secondary phase has formed along the length of the palygorskite crystals with an interface parallel to {010} of the palygorskite. The resulting grain structures have an elongate 'wing-like' morphology. Parallel intergrowths of palygorskite crystals that are joined along the [010] direction to form 'raft-like' bundles are also common (Figure 5). These raft-like bundles are a common feature of the microfabric of the clay before disaggregation (Krekeler *et al.*, 2004).

Transmission electron microscopy

We can obtain ion-milled samples without significant sample damage for palygorskite-sepiolite minerals. However, these minerals are sensitive to an electron beam. Features similar to those in Figure 6 were common, but difficult to obtain, even for exposure times of <0.7 s. Structural damage occurred before selected area electron diffraction could be obtained; thus, diffraction patterns are unavailable for a given image.

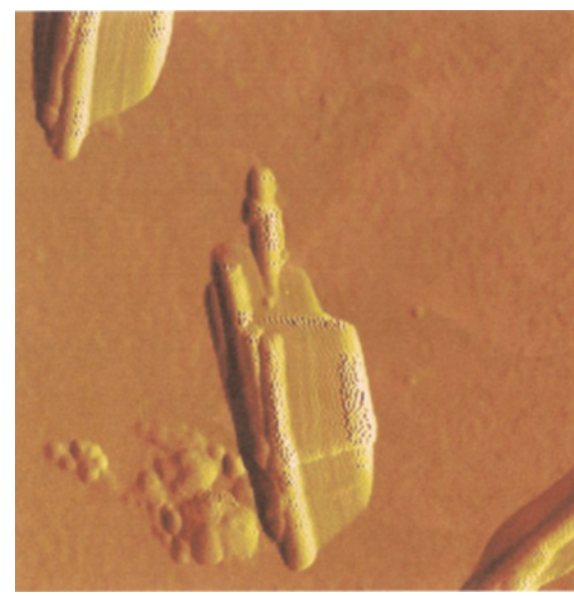


Figure 4. AFM image (deflection data) of smectite overgrowth on palygorskite from the tan clay dispersed on a mica substrate.

https://doi.org/10.1346/CCMN.2005.0530109 Published online by Cambridge University Press

Figure 6a shows a TEM image from the tan clay at 125 cm above the contact with the blue clay. There are three structural domains in this image: (1) parallel to sub-parallel lattice-fringe lines; (2) poorly resolved spots arranged in a regular or nearly regular manner to form rectangular blocks; and (3) amorphous regions. The amorphous regions (bottom and upper left), show no linear aspects and indicate that the TEM image was properly stigmated.

Parallel to sub-parallel lattice-fringe lines occur in the upper, central left and lower portion of the image and have a spacing of ~13.0 Å. These are interpreted as smectite; the 13.0 Å spacing is consistent with the exchange with LRW (Kim *et al*., 1995). Rectangular blocks (black, indicating electron density) occur in the central right portion of the image and the widths of these blocks vary, at 10.4, 14.8, 16.9, 21.7 and 24.5 Å (labeled in Figure 6b). The heights of rectangular blocks also vary. The narrower blocks, (10.4 Å and 14.8 Å, are ~7.6 Å in height, and the wider blocks (16.9, 21.7 and 24.5 Å) 5.8–6.0 Å high. Blocks are shifted 6.5 to 7.2 Å in the [001] direction with respect to each other. The rectangular blocks are interpreted as palygorskite/sepiolite polysomes (or ribbons of 2:1 layers) of variable width. The widths are consistent with double tetrahedral chains (10.4 Å), triple tetrahedral chains (14.8 Å), quadruple tetrahedral chains (21.7 Å), and quintuple tetrahedral chains (24.5 Å). Note that the 16.9 Å width is intermediate between triple and quadruple chain widths. The central portion of the TEM image shows a region where parallel to sub-parallel lattice-fringe lines and rectangular blocks are intergrown, suggesting an overgrowth of smectite on palygorskite-sepiolite.

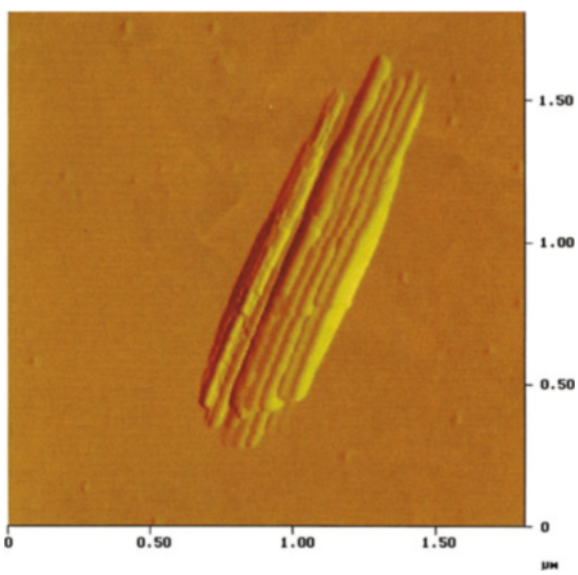


Figure 5. AFM image (deflection data) of a palygorskite 'raft' from the blue clay dispersed on a mica substrate.

Eighteen palygorskite fibers and eight smectite particles (representative analyses are given in Table 1) were analyzed using EDS. Particles were selected for analysis to avoid underlying particles or multiple particles. All EDS analyses were obtained at 400,000 × and data are reported normalized to 100 wt.%. The analyses show that smectite and palygorskite in the tan clay are similar in chemical composition, although there are some statistically significant differences. The SiO_2, TiO_2, Fe_2O_3 and MgO data were analyzed using a two-sample t-test with the 18 palygorskite and eight smectite analyses. The SiO_2, TiO_2 and Fe_2O_3 concentrations in palygorskite and smectite are not statistically different. However, concentrations are statistically different for MgO ($p = 0.00038$)

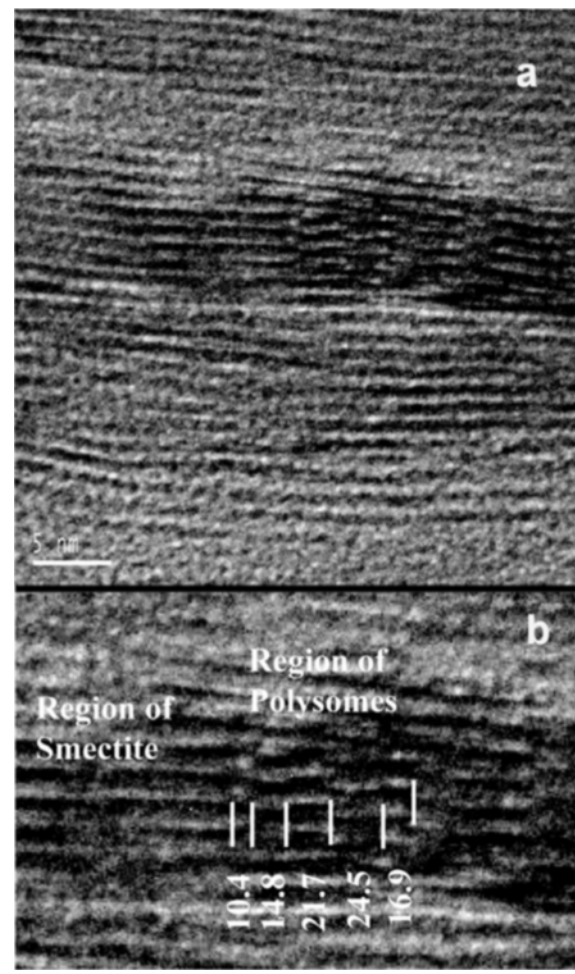


Figure 6. TEM image of palygorskite-smectite intergrowth. (a) Unlabeled image with parallel to sub-parallel lattice fringes (smectite) in the upper, central left, and lower portions of the image and rectangular blocks arranged in a regular or nearly regular manner (ribbons) in the center right portion of the image. (b) Enlargement of the transition zone between smectite and palygorskite with features labeled. Labels of ribbons given in Ångstroms. The image is approximately along the [100] direction of the palygorskite crystal.

https://doi.org/10.1346/CCMN.2005.0530109 Published online by Cambridge University Press

Table 1. Representative EDS analyses of palygorskite and smectite from the tan clay 125 cm above the contact with the blue clay.

	Palygorskite analyses					Smectite analyses				
	1	2	3	4	5	1	2	3	4	5
SiO_2	64.05	61.29	65.17	66.10	69.58	60.13	66.01	67.05	63.64	64.01
TiO_2	3.55	0.09	0.10	0.09	1.06	0.27	0.07	0.12	0.00	5.13
Al_2O_3	8.48	22.04	16.16	14.20	10.38	23.00	19.12	17.23	21.40	13.07
Fe_2O_3	5.79	5.57	6.11	6.49	6.71	5.65	5.32	5.31	6.22	6.96
MgO	13.80	6.56	9.62	10.38	10.71	6.51	7.55	8.51	5.59	9.12
MnO	0.07	0.03	0.06	0.07	0.17	0.04	0.01	0.10	0.07	0.07
CaO	3.78	1.97	1.73	1.58	0.93	0.77	1.17	0.85	1.25	0.67
K_2O	0.15	1.68	0.56	0.62	0.34	2.26	0.21	0.20	1.28	0.56
Na_2O	0.33	0.77	0.49	0.47	0.12	1.37	0.54	0.63	0.55	0.41
$Total_{norm.}$	100.00	100.00	100.00	100.00	100.00	100.00	100.00	100.00	100.00	100.00

and Al_2O_3 ($p = 0.02319$) in smectite *vs*. palygorskite. The MgO concentrations are greater in palygorskite, with a difference between the averages of 2.77 wt.%. The Al_2O_3 concentrations are greater in smectite, with a difference between the averages of 3.33 wt.%.

DISCUSSION

Based on the observed micromorphology and microtopography of samples, TEM lattice-fringe images and compositional analyses of crystals from the tan clay, a reaction mechanism sequence for the transformation of palygorskite to smectite in the Pittman Quarry is evident. The change in palygorskite from well formed crystals with smooth and continuous faces (Figures 1,2) to a rough, hummocky microtopography (Figure 3) suggests partial dissolution. Similar features were observed by TEM in the transformation experiments of Golden *et al*. (1985). The platy 'wing-like' features, which are only observed in the tan clay on shortened palygorskite crystals with a hummocky microtopography, indicate precipitation of a secondary phase with a different structure from pre-existing dissolved silica-rich material (Figures 3,4). The platy morphology is suggestive of another layer silicate that through TEM and EDS data has been identified as a smectite, ferrian montmorillonite (Figures 3,4). The EDS analyses of discrete palygorskite and smectite particles indicate that these minerals in the tan clay are similar in chemical composition, although palygorskite is enriched in Mg and smectite is slightly enriched in Al. The similarity in chemical composition as well as the structural similarity between polysomes and 2:1 layer silicates may explain why the intergrowth of smectite and palygorskite is so common in the tan clay as the chemical composition of 2:1 layers changes little. The formation of 'wings' on the palygorskite crystals by the smectite overgrowths is consistent with the SEM observations of the initial alteration products made by Merkl (1989). Kaolinite and illite grains within the sample also display overgrowths of smectite (Figure 3; and Krekeler *et al*., 2004).

On all of the 'winged' palygorskite crystals observed by AFM, a specific crystallographic orientation between the smectite overgrowth and the palygorskite is evident. The smectite layers on either side of a single palygorskite crystal are coplanar and run the length of the palygorskite. Smectite overgrowths are found in no other orientation about the palygorskite [100] zone axis. These morphological data and the TEM lattice-fringe data indicate an epitaxial relationship between the smectite and palygorskite. After partial palygorskite dissolution, smectite nucleated heterogeneously on the palygorskite such that the smectite 2:1 layers are parallel to the 2:1 layer ribbons of palygorskite. This epitaxial relationship is described as {010} [001] palygorskite || {010} [001] smectite (Figure 7).

The double to quintuple tetrahedral chain-width polysomes in palygorskite fibers are similar to polysome-width variation in sepiolite and yofortiterite (Krekeler and Guggenheim, 2005). The occurrence of these defects in sedimentary palygorskite-sepiolite minerals along with samples from other low-temperature environments investigated by Krekeler and Guggenheim (2005) suggests that they may be common.

CONCLUSIONS

This study provides the first direct evidence of a transformation of palygorskite to smectite, and indicates that the mechanism of the transformation is dissolution of the palygorskite with coeval nucleation and growth of smectite on the palygorskite in an epitaxial relationship. In the region where the transformation occurs, the widths of polysomes are variable in the [010] direction; variations are consistent with ribbons containing double tetrahedral-chain to quintuple tetrahedral-chain widths.

Merkl (1989) proposed that transformations occurred after initial deposition of the palygorskite deposits in response to interactions with oxidizing meteoric groundwaters. Our TEM results are consistent with alteration after deposition. However, precipitation of palygorskite-smectite intergrowths as original chemical precipitates

https://doi.org/10.1346/CCMN.2005.0530109 Published online by Cambridge University Press

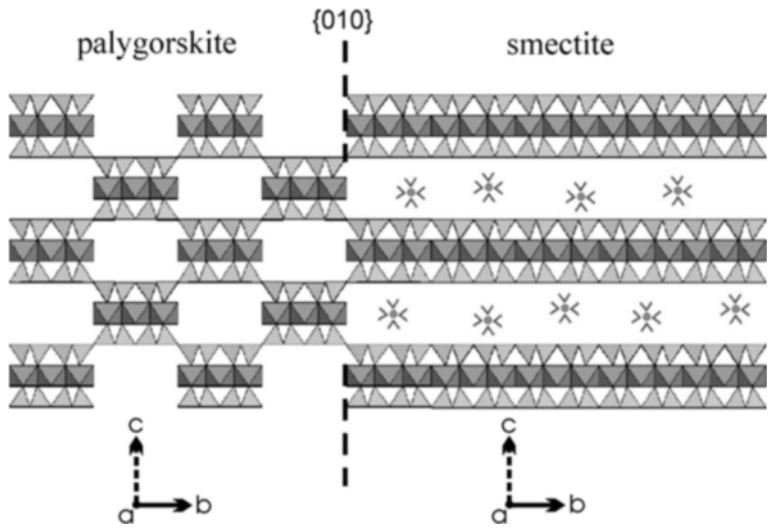


Figure 7. Structural schematic of the epitaxial relationship between palygorskite and smectite overgrowths; {010} [001] palygorskite || {010} [001] smectite.

from the water column cannot be ruled out. A potential geological significance of particles with these transformations in sediments is that they may prove to be a paleoenvironmental indicator of specific geochemical conditions as is the presence of palygorskite and sepiolite.

We have not, however, defined the precise conditions under which this transformation occurs, for example, the possible roles of Fe oxidation or pH. In addition, we have not presented calculated images to match our observed images, because the observed images deteriorated quickly in the electron beam; we have had to rely on interpretations from lattice-fringe images and AFM images.

ACKNOWLEDGMENTS

We thank J. Cuevas, Universidad Autónama de Madrid, Spain, and H. Lindgreen, Geological Survey of Denmark and Greenland, for their reviews. This work was funded through the National Science Foundation, under grants EAR-0001122, EAR-0308588, and EAR-0001251.

REFERENCES

Bickmore, B., Bosbach, D., Hochella, M.F. Jr., Charlet, L. and Rufe, E. (2001) In situ atomic force microscopy study of hectorite and nontronite dissolution: Implications for phyllosilicate edge surface structures and dissolution mechanisms. *American Mineralogist*, **86**, 411–423.

Galán, E. (1996) Properties and applications of palygorskite-sepiolite clays. *Clay Minerals*, **31**, 443–453.

Golden, D.C. and Dixon, J.B. (1990) Low temperature alteration of palygorskite to smectite. *Clays and Clay Minerals*, **38**, 401–408.

Golden, D.C., Dixon, J.B., Shadfar, H. and Kippenberger, L.A. (1985) Palygorskite and sepiolite alteration to smectite under alkaline conditions. *Clays and Clay Minerals*, **33**, 44–50.

Güven, N. and Carney, L.L. (1979) The transformation of sepiolite to stevensite and the effect of added chloride and hydroxide. *Clays and Clay Minerals*, **27**, 253–260.

Jones, B. and Galán, E. (1988) Sepiolite and palygorskite. Pp. 631–674 in: *Hydrous Phyllosillicates* (S.W. Bailey, editor). Reviews in Mineralogy, **19**. Mineralogical Society of America, Washington, D.C.

Khoury, H.H., Eberl, D.D. and Jones, B.F. (1982) Origin of magnesium clays from the Amargosa desert, Nevada. *Clays and Clay Minerals*, **30**, 327–336.

Kim, J., Peacor, D.R., Tessier, D. and Elass, F. (1995) A technique for maintaining texture and permanent expansion of smectite interlayers for TEM observations. *Clays and Clay Minerals*, **43**, 51–57.

Krekeler, M. and Guggenheim, S. (2005) Defects in microstructure in palygorskite-sepiolite minerals: A transmission electron microscopy (TEM) study. *American Mineralogist*, (in review).

Krekeler, M., Guggenheim, S. and Rakovan, J. (2004) A microtexture study of palygorskite-rich sediments from the Hawthorne Formation, southern Georgia, by transmission electron microscopy and atomic force microscopy. *Clays and Clay Minerals*, **52**, 263–274.

Leguey, S., Martin-Rubi, J.A., Casas, J., Marta, J., Cuevas, J., Alvarez, A. and Medina, J.A. (1995) Diagenetic evolution and mineral fabric in sepiolitic materials from the Vicalvaro deposit (Madrid Basin). Pp. 383–392 in: *Clays Controlling the Environment* (G.J. Churchman, R.W. Fitzpatrick and R.A. Eggleton, editors). Proceedings of the 10th International Clay Conference, Adelaide, Australia, 1993. CSIRO Publishing, Melbourne, Australia,

Merkl, R.S. (1989) A sedimentological, mineralogical, and geochemical study of the fuller's earth deposits of the Miocene Hawthorne group of south Georgia-north Florida. PhD dissertation, Indiana University, Bloomington, Indiana 182 pp.

Nagy, K.L. and Blum, A.E., editors (1994) *Scanning Probe Microscopy of Clay Minerals*. Workshop Lectures, **7**, The Clay Minerals Society, Boulder, Colorado, 239 pp.

Patterson, S.H. (1974) *Fuller's earth and industrial mineral resources of the Meigs-Attapulgus-Quincy district, Georgia and Florida*. U.S. Geological Survey Professional Paper: Report P0828, 45 pp.

Randall, B.A.O. (1956) Stevensite from the Whin Sill in the region of the North Tyne. *Mineralogical Magazine*, **32**, 218–229.

https://doi.org/10.1346/CCMN.2005.0530109 Published online by Cambridge University Press

Weaver, C.E. (1984) Origin and geologic implications of the palygorskite deposits of the S.E. United States. Pp. 39–58 in: *Palygorskite-Sepiolite: Occurrences, Genesis, and Uses* (A. Singer and E. Galán, editors). Developments in Sedimentology, **37**. Elsevier, New York.

Weaver, C.E. and Beck, K.C. (1977) *Miocene of the S.E. United States: a model for chemical sedimentation in a perimarine environment*. Developments in Sedimentology, **22**, Elsevier, New York, 234 pp.

(*Received 26 February 2004; revised 7 September 2004; Ms. 886; A.E. Ray E. Ferrell, Jr.*)

https://doi.org/10.1346/CCMN.2005.0530109 Published online by Cambridge University Press